



Published in final edited form as:

*Circ Res.* 2021 January 22; 128(2): 246–261. doi:10.1161/CIRCRESAHA.120.317452.

## Intracellular $\beta_1$ -Adrenergic Receptors and Organic Cation Transporter 3 Mediate Phospholamban Phosphorylation to Enhance Cardiac Contractility

Ying Wang<sup>#a</sup>, Qian Shi<sup>#a,1</sup>, Minghui Li<sup>a,b</sup>, Meimi Zhao<sup>a,c</sup>, Raghavender Reddy Gopireddy<sup>a</sup>, Jian-Peng Teoh<sup>a</sup>, Bing Xu<sup>a,d</sup>, Chaoqun Zhu<sup>a</sup>, Kyle E. Ireton<sup>a</sup>, Sanghavi Srinivasan<sup>a</sup>, Shaoliang Chen<sup>b</sup>, Paul J. Gasser<sup>e</sup>, Julie Bossuyt<sup>a</sup>, Johannes W. Hell<sup>a</sup>, Donald M. Bers<sup>a</sup>, Yang K. Xiang<sup>a,d</sup>

<sup>a</sup>Department of Pharmacology, University of California at Davis, Davis, CA 95616;

<sup>b</sup>Nanjing First Hospital, Nanjing Medical University, Nanjing 211166, China;

<sup>c</sup>Department of Pharmaceutical Toxicology, China Medical University, Shenyang, 110122, China;

<sup>d</sup>VA Northern California Health Care System, Mather, CA 95655,

<sup>e</sup>Department of Biomedical Sciences, Marquette University, Milwaukee, WI 53201;

# These authors contributed equally to this work.

### Abstract

**Rationale:**  $\beta_1$ -adrenoceptors ( $\beta_1$ ARs) exist at intracellular membranes and Organic Cation Transporter 3 (OCT3) mediates norepinephrine entry into cardiomyocytes. However, the functional role of intracellular  $\beta_1$ AR in cardiac contractility remains to be elucidated.

**Objective:** Test localization and function of intracellular  $\beta_1$ AR on cardiac contractility.

**Methods and Results:** Membrane fractionation, super-resolution imaging, proximity ligation, co-immunoprecipitation and single-molecule pulldown demonstrated a pool of  $\beta_1$ ARs in mouse hearts that was associated with sarco/endoplasmic reticulum  $\text{Ca}^{2+}$ -ATPase at the sarcoplasmic reticulum (SR). Local protein kinase A (PKA) activation was measured using a PKA biosensor targeted at either the plasma membrane (PM) or SR. Compared to wild type (WT), myocytes lacking OCT3 (OCT3KO) responded identically to the membrane-permeant  $\beta$ AR agonist

---

**Address correspondence to:** Dr. Yang K. Xian, Department of Pharmacology, 2426 Tupper Hall, One Shields Ave., University of California at Davis, Davis, CA 95616, USA, Tel: 5307529206, ykxiang@ucdavis.edu.

<sup>1</sup>Present address: Fraternal Order of Eagles Diabetes Research Center, Division of Endocrinology and Metabolism, Roy J. and Lucille A. Carver College of Medicine, University of Iowa, Iowa City, Iowa 52242

**Publisher's Disclaimer:** This article is published in its accepted form. It has not been copyedited and has not appeared in an issue of the journal. Preparation for inclusion in an issue of *Circulation Research* involves copyediting, typesetting, proofreading, and author review, which may lead to differences between this accepted version of the manuscript and the final, published version.

#### DISCLOSURES

None.

#### SUPPLEMENTAL MATERIALS

Expanded Materials & Methods

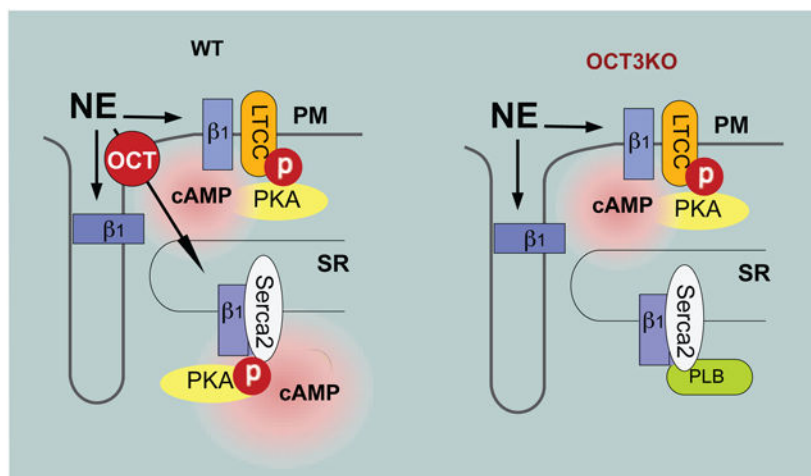
Online Figures I–XIII

References<sup>17–20, 32–38</sup>

isoproterenol in PKA activation at both PM and SR. The same was true at the PM for membrane-impermeant norepinephrine, but the SR response to norepinephrine was suppressed in OCT3KO myocytes. This differential effect was recapitulated in phosphorylation of the SR-pump regulator phospholamban. Similarly, OCT3KO selectively suppressed calcium transients and contraction responses to norepinephrine, but not isoproterenol. Furthermore, sotalol, a membrane-impermeant  $\beta$ AR-blocker suppressed isoproterenol-induced PKA activation at the PM, but permitted PKA activation at the SR, phospholamban phosphorylation and contractility. Moreover, pretreatment with sotalol in OCT3KO myocytes prevented norepinephrine induced PKA activation at both PM and the SR and contractility.

**Conclusion:** Functional  $\beta_1$ ARs exists at the SR and is critical for PKA-mediated phosphorylation of phospholamban and cardiac contractility upon catecholamine stimulation. Activation of these intracellular  $\beta_1$ ARs requires catecholamine transport via OCT3.

### Graphical Abstract



### Keywords

Beta-1 adrenergic receptor ( $\beta_1$ AR);  $\beta$ -blockers; phospholamban (PLB); cardiac contractility and energetics; catecholamine; Organic Cation Transporter 3 (OCT3); adrenergic receptor

### Subject Terms:

Basic Science Research; Calcium Cycling/Excitation-Contraction Coupling; Cell Signaling/Signal Transduction; Contractile Function

## INTRODUCTION

Plasma membrane receptors are major mechanisms by which cells respond to extracellular stimuli, allowing cells to adapt to their surrounding environments and to modulate tissue/organ function in reaction to changes of neurohormones. Non-steroid hormones signal mainly through receptors at the plasma membrane (PM) to regulate cellular function. This includes sympathetic regulation of cardiac function via adrenergic receptors (ARs) on the

PM of cardiomyocytes. Recently, a complementary thread of studies has found that neurotransmitters, peptide hormones, and growth factors also act on intracellular membrane receptors.<sup>1–4</sup> Accumulating data indicate that intracellular G-protein coupled receptors (GPCRs) located at different organelles, e.g., mitochondria,<sup>5</sup> endoplasmic reticulum membranes<sup>6</sup> and Golgi,<sup>7</sup> can be activated inside the cells and induce location-specific effects. The development of these observations helps expanding the current understanding of hormonal regulation of cardiac function.

$\beta_1$ ARs, a prototype GPCR, acts as a linchpin of sympathetic regulation in the heart and has been demonstrated to be localized and activated intracellularly in cardiomyocytes.<sup>8</sup> However, the role of intracellular  $\beta_1$ ARs in the regulation of cardiac excitation-contraction is still unknown. During the fight or flight response, activation of the sympathetic nerve and adrenal glands releases catecholamines (epinephrine, EPI and norepinephrine, NE) to activate  $\beta$ ARs on myocytes, and thus enhance heart rate, cardiac contraction and relaxation.<sup>9, 10</sup> These effects involve  $\beta$ ARs stimulation-dependent cAMP and subsequent activation of protein kinase A (PKA) to enhance substrate phosphorylation. The PKA phosphorylation of different substrates occurs in different spatiotemporal nanodomains including L-type  $\text{Ca}^{2+}$  channel (LTCC) at the PM, phospholamban (PLB) and ryanodine receptor type 2 (RyR2) on the SR, and troponin I (TnI) and myosin binding protein C (MYBP-C) on the myofilaments.<sup>11, 12</sup>

Both NE and EPI are vital neurohormones in physiological stress responses. However, EPI and NE have extremely hydrophilic octanol/water partition coefficients ( $\text{LogP} = -1.37$  and  $-1.24$ , respectively, <https://pubchem.ncbi.nlm.nih.gov>). After release from nerve termini, a small portion of catecholamine can enter myocytes, primarily mediated by corticosterone-sensitive organic cation transporter 3 (OCT3, also named extra-neuronal monoamine transporter, EMT).<sup>2, 13</sup> OCT3-mediated NE uptake is necessary for activation of intracellular ARs in cardiomyocytes, including both nuclear  $\alpha_1$ ARs and Golgi-localized  $\beta_1$ ARs.<sup>2, 8</sup> Intriguingly, decreased NE uptake into myocardium and cardiac NE contents in heart failure patients are associated with significantly blunted inotropy response.<sup>14</sup> In dilated cardiomyopathy patients, OCT2 expression is reduced and predicts the impairment of cardiac function.<sup>15</sup> However, the functional role of NE uptake facilitated by OCT3 in adrenergic stimulation of cardiac contractile is unclear.

Activation of  $\beta_1$ ARs induces spatial, temporal segregated cAMP-PKA signals in heart.<sup>12, 16</sup> The application of Förster resonance energy transfer (FRET)-based biosensors have been instrumental in the investigation and dissection of compartmentalized cAMP/PKA signaling on the nanodomain scale.<sup>12, 17, 18</sup> By using genetically encoded biosensors, previous studies from our group and others found that compartmentalized cAMP/PKA signal generated in response to  $\beta$ AR stimulation differs at the PM and SR local domains in both amplitude and kinetics.<sup>12, 17</sup> The mechanism underlying this heterogeneity is still unclear. We hypothesize that a population of  $\beta_1$ ARs is located near or at the SR and plays an important role in modulating calcium ( $\text{Ca}^{2+}$ ) cycling and cardiac contractility. In this study, we tested the expression, activation and functional effects of SR-localized  $\beta_1$ AR in cardiac contractility. Our results provide novel insights into the localization and regulation of intracellular  $\beta_1$ AR, therefore, offering potential and precise target for  $\beta_1$ AR-associated therapeutic strategies.

## METHODS

### Data Availability.

The data, analytic methods, and study materials are made available to other researchers for purposes of reproducing the results or replicating the procedure. Please see the Major Resources Table and Expanded Materials & Methods in the Online Data Supplement.

All experiments including animal feeding, treatment, and tissue collection were approved by the Institutional Animal Care and Use Committees (protocol: 20234 and 20957) of the University of California at Davis and follow NIH guidelines. Male and female 2–4-month-old C57/BL6 and OCT3KO, newborn  $\beta_1$ AR-KO,  $\beta_2$ AR-KO and  $\beta_1\beta_2$ AR-KO mice were described previously.<sup>17, 19</sup> Male Sprague Dawley outbred rats and New Zealand white rabbits were used in this study.

## RESULTS

### Existence and distribution of a distinct pool of $\beta_1$ AR at the SR in cardiomyocytes.

To examine the existence of different subcellular pools of  $\beta_1$ ARs in adult mouse hearts, we fractionated heart tissues to separate the PM from intracellular membrane compartments. Sarcoplasmic endoplasmic reticulum  $\text{Ca}^{2+}$ -ATPase 2 (SERCA2) and ryanodine receptor 2 (RyR2), which are SR resident proteins, were used as markers for the intracellular membrane fraction (non-PM), and insulin receptor (InsR) and lack of SERCA2/RyR2 were used to identify PM fraction.  $\beta_1$ ARs were clearly detected in both PM and intracellular membrane fractions (non-PM) in WT mouse hearts, but not in  $\beta_1$ AR-KO mouse hearts (Figure 1A and Online Figure IA), indicating that endogenous  $\beta_1$ AR exists in at least two different pools in mouse hearts. In addition, quantitative radioligand-binding assay measured the functional  $\beta_1$ ARs that bind to [ $^{125}$ I] radio-labeled cyanopindolol in both PM and intracellular membrane fractions (Figure 1B), supporting the existence of an intracellular pool of functional  $\beta_1$ ARs in hearts. We also applied a fluorescence dye BODIPY-tagged  $\beta$ AR antagonist propranolol (FL-Prop) to stain endogenous  $\beta_1$ ARs in mouse adult ventricle myocytes (AVMs). Confocal images of FL-Prop fluorescent staining in WT mouse AVMs showed a distribution of  $\beta$ ARs on both surface membrane and intracellular space (Online Figure IB), which was abrogated by addition of 1  $\mu\text{mol/L}$  and 10  $\mu\text{mol/L}$  propranolol (Online Figure IB). Moreover, compared with WT and  $\beta_2$ AR-KO cardiomyocytes, the fluorescent dots and intensity of FL-Prop were greatly reduced in the  $\beta_1$ AR-KO and  $\beta_1\beta_2$ AR-KO cardiomyocytes (Online Figure IC–D), indicating that FL-Prop mainly stains endogenous  $\beta_1$ AR.

SR localized  $\text{Ca}^{2+}$  cycling proteins such as SERCA2 and RyR2 are crucial for the modulation of cardiac contractility in response to  $\beta$ AR activation.<sup>11</sup> We hypothesize that a population of intracellular  $\beta_1$ ARs are present at the SR. We examined a potential colocalization of overexpressed  $\beta_1$ AR with SERCA2 or RyR2.  $\beta_1$ AR displayed specific colocalization with SERCA2, but not RyR2, in mouse AVMs (Figure 1C–E and Online Figure IIA). As controls, overexpressed  $\beta_2$ AR did not display overlap with either SERCA2 or RyR2 (Online Figure IIIA–B). Next, we applied proximity ligation assay (PLA) to further explore the proximal relationship between  $\beta_1$ AR and SERCA2. We detected robust PLA

signals in mouse AVMs co-stained for  $\beta_1$ AR and SERCA2, suggesting that these  $\beta_1$ ARs and SERCA2 are at 40 nm or less apart. Conversely, PLA signals were not detected after co-staining with antibodies against  $\beta_1$ AR and IgG or against  $\beta_1$ AR and RyR2 and only a small amount of PLA signals was detected after co-staining for  $\beta_1$ AR and junctophilin 2 (JP2) (Figure 1F and Online Figure IIB–D). Moreover, endogenous  $\beta_1$ AR was pulled down with  $\beta_1$ AR antibody (Figure 1G). We found that both SERCA2 and its regulatory protein, phospholamban (PLB), were co-immunoprecipitated with the endogenous  $\beta_1$ ARs. In contrast, RyR2 was not observed in the immunoprecipitation. Furthermore, we applied a super-sensitive single molecule pull down (SiMPull) assay<sup>20</sup> to visualize individual  $\beta_1$ AR-SERCA2 complex in heart lysate. Figure 1H shows that  $\beta_1$ AR antibody was able to pull down a significant amount of SERCA2 molecules compared to control IgG antibody. Together, these data demonstrate that a population of  $\beta_1$ ARs is localized at the SR and forms a complex with SERCA2 in AVMs.

### **Organic Cation Transporter 3 (OCT3) is required to activate the pool of $\beta_1$ ARs by catecholamine at the SR.**

$\beta$ -adrenoceptor stimulation results in activation of PKA, a key mediator for phosphorylating multiple  $\text{Ca}^{2+}$  handling proteins (e.g. PLB).<sup>21</sup> To directly assess PKA activity induced by the SR-localized  $\beta_1$ AR, we employed a genetically encoded Förster resonance energy transfer (FRET)-based A kinase activity reporter (AKAR) that is anchored at the intracellular SERCA2 complex on the SR (SR-AKAR3).<sup>17, 18</sup> In comparison, the PKA activity induced by the PM-localized  $\beta_1$ AR was assessed by an AKAR3 anchored on the PM (PM-AKAR3).

Previous studies showed that OCT3-mediated transportations of EPI or NE into cells are essential for activating intracellular adrenergic receptors in cardiomyocytes.<sup>2, 8</sup> Here, we used mice with genetic deletion of OCT3 to examine the impacts of OCT3 on subcellular PKA activity induced by PM- or SR-localized  $\beta_1$ AR (PM- $\beta_1$ AR or SR- $\beta_1$ AR). Unlike endogenous catecholamines, isoproterenol (ISO, LogP = 1.4) and dobutamine (LogP = 3.6), two membrane permeant  $\beta$  agonists, activate internal  $\beta$ AR via passive diffusion into myocytes (Figure 2A–B).<sup>7</sup> Therefore, deleting OCT3 should selectively block the access of NE and EPI but not ISO and Dob to SR-localized  $\beta_1$ AR (Figure 2A–B). NE, EPI, ISO and Dob all induced robust PKA activity at both the PM and SR in WT myocytes (Online Figure IVA–D). The kinetics of ligand induced PKA activity at the PM were comparable but were faster than those at the SR (Online Figure IVA–E). Among the SR-PKA activity, the Dob induced increases were faster than those by ISO, EPI and NE, consistent with its faster membrane permeability (Online Figure IV A–E). As predicted, the ISO-induced PKA activity at both the PM and SR was not affected by deletion of OCT3 (Figure 2C–D). However, deletion of OCT3 selectively attenuated NE-induced PKA activity at the SR without affecting PKA activity at the PM (Figure 2E–F). Moreover, inhibition of  $\beta_1$ AR with CGP20712a completely abolished PKA activity induced by NE and ISO at both PM and the SR in AVMs whereas inhibition of  $\beta_2$ AR with ICI118551 did not affect these PKA activities (Online Figure IV F–I). These observations were not due to change in  $\beta_1$ AR expression in OCT3-KO hearts (Online Figure V). Additionally, we have examined PKA activity at the myofilaments (MF) with an AKAR3 anchored on the troponin complex (MF-AKAR3<sup>18</sup>), which is adjacent to the SR. Our data show deletion of OCT3 selectively attenuated NE but

not ISO induced PKA activity on the myofilaments (Online Figure VA). To explore specific PKA substrate affected by SR-localized  $\beta_1$ AR activation, we then examined PKA phosphorylation of phospholemman (PLM, Ser<sup>63</sup>) and LTCC (Ser<sup>1928</sup>) at the PM, PLB (Ser<sup>16</sup>) and RyR2 (Ser<sup>2808</sup>) at the SR, TnI (Ser<sup>23/24</sup>) and MyBPC (Ser<sup>282</sup>, Ser<sup>273</sup>, Ser<sup>302</sup>) at myofilament. Deletion of OCT3 selectively attenuated NE-induced PKA phosphorylation of PLB and TnI without affecting PKA phosphorylation of PLM, LTCC, RyR2, and MyBPC (Figure 2G–H and Online Figure V B–H). In comparison, ISO-induced PKA phosphorylation of both PLM and PLB were not affected by OCT3 deficiency (Figure 2G–H). These data suggest that deletion of OCT3 blocks catecholamine-dependent activation of the  $\beta_1$ ARs at the SR and the myofilament and downstream PKA-dependent PLB and TnI phosphorylation.

### Functional consequences of the internal pool of $\beta_1$ ARs on adult ventricular myocyte.

We then assessed whether the deletion of OCT3 affects catecholamine induced  $Ca^{2+}$  handling and sarcomere shortening (SS) in isolated AVMs. Compared with basal conditions, stimulation with different  $\beta$ AR agonists (ISO, Dob, NE, and EPI) led to increased SS and  $Ca^{2+}$  transient amplitude, and decreased  $Ca^{2+}$  decay tau in both WT and OCT3KO AVMs (Figure 3A–H and Online Figure VIA–K). Dob induced a faster inotropic response than ISO and NE in WT AVMs. The increases in E-C coupling were blocked by  $\beta_1$ AR antagonist CGP20712a, but not affected by  $\beta_2$ AR inhibition with ICI118551 (Online Figure VII). Deletion of OCT3 did not affect ISO- or Dob-induced inotropic responses (Figure 3A–D and Online Figure VID–K). Conversely, the NE- and EPI-promoted responses in contraction,  $Ca^{2+}$  transients and  $[Ca^{2+}]_i$  decay tau were significantly attenuated in OCT3KO vs WT AVMs (Figure 3E–H and Online Figure VIJ–K). Deletion of OCT3 also shifted the NE dose-response curve of SS to the right without affecting ISO-induced dose-response curve (Figure 3I–J).

To independently test the role of OCT3 in the SR-located  $\beta_1$ AR/PKA signaling, we applied an OCT3/EMT inhibitor corticosterone (CORTI) to prevent NE transport into myocytes (Figure 4A–B). While CORTI had minimal effect on NE-induced PKA activity at the PM domain, it significantly attenuated NE-induced PKA activity at the SR domain (Figure 4C–D). CORTI did not change ISO-induced PKA activity at either the PM or SR domain in rat AVM (Figure 4C–D). In agreement, CORTI significantly reduced NE- but not ISO-induced PKA phosphorylation of PLB at Ser<sup>16</sup> (Figure 4E–F). CORTI also significantly attenuated NE-induced increases in contractility,  $Ca^{2+}$  transient amplitude, and rate of  $Ca^{2+}$  transient decay (Figure 4G–I). However, these CORTI effects were absent in the responses to ISO stimulation (Figure 4J–L). Together, these data suggest that OCT3-dependent transport is required for stimulation of SR-localized  $\beta_1$ AR/PKA/PLB signal cascade for optimal increases in  $Ca^{2+}$  handling and contractility.

### Activation of the internal $\beta_1$ ARs at the SR was not blocked by membrane impermeant $\beta$ -blockers.

Sotalol, a membrane impermeant  $\beta$ -blocker (LogP = 0.24), has limited access to intracellular  $\beta_1$ AR.<sup>22</sup> To further dissect the physiological function of the SR- $\beta_1$ AR, we applied sotalol to selectively block the PM- $\beta_1$ AR but permit access and activation of SR- $\beta_1$ AR by agonists. In

contrast, propranolol, a membrane permeant  $\beta$ -blocker ( $\text{LogP} = 3.48$ ), is expected to block  $\beta$ ARs both on the PM and at intracellular membranes (Online Figure VIIIA). We tested the accessibilities of sotalol and propranolol to the  $\beta_1$ ARs by examining their abilities to compete with fluorescent BODIPY-tagged propranolol (Fl-Prop) from binding to  $\beta_1$ ARs. Confocal images of Fl-Prop fluorescent staining in WT mouse AVMs showed a distribution of  $\beta$ AR on both surface and intracellular membranes (Online Figure VIIIB). Sotalol pretreatment did not block the intracellular staining (Online Figure VIIIB); whereas addition of propranolol effectively competed against Fl-Prop from binding to  $\beta_1$ AR in AVMs (Online Figure VIIIB). Addition of ISO and NE also effectively competed against Fl-Prop from binding to  $\beta_1$ AR in AVMs. Thus, intracellular  $\beta_1$ AR can be blocked by membrane permeant  $\beta$ -blockers but are less accessible to membrane impermeant  $\beta$ -blockers.

Sotalol was then applied to isolate PKA activity induced by local compartmentalized  $\beta_1$ AR at the SR (Figure 5A–C). In WT,  $\beta_1$ AR-KO and  $\beta_2$ AR-KO mouse neonatal myocytes and WT mouse, rat, and rabbit AVMs, sotalol readily inhibited ISO induced and  $\beta_1$ AR mediated PKA activity at the PM, but not those at the SR (Figure 5D–G, Online Figure IXA–D and Online Figure X). In rat AVMs, the  $\text{IC}_{50}$  of sotalol for inhibition of ISO-induced PKA activity at the SR was about 10-fold higher than that of PKA activity at the PM (Figure 5G, PM-AKAR3  $\text{IC}_{50} = 2.22 \pm 0.06 \mu\text{mol/L}$ ; SR-AKAR3  $\text{IC}_{50} = 21.5 \pm 0.06 \mu\text{mol/L}$ ). In contrast, the membrane permeant  $\beta$ -blocker propranolol inhibited ISO-induced PKA activity at both the PM and SR in a concentration-dependent manner (Figure 5F, PM-AKAR3  $\text{IC}_{50} = 74.0 \pm 0.05 \text{ nmol/L}$ , SR-AKAR3  $\text{IC}_{50} = 99.2 \pm 0.06 \text{ nmol/L}$ ). Another poorly permeant  $\beta$ -blocker, atenolol ( $\text{LogP} = 0.6$ ), acted similarly to sotalol by selectively inhibiting ISO-induced PKA activity only at the PM in rat AVMs (Online Figure IXE–F). In comparison, membrane permeant carvedilol ( $\text{LogP} = 4.19$ ) inhibited ISO-induced PKA activity at both the PM and the SR (Online Figure IXE–F). Together, these data support that local activation of SR- $\beta_1$ AR-PKA signaling was minimally suppressed by membrane impermeant  $\beta$ -blockers, a conserved mechanism throughout different cardiac myocytes from different species. This also indicates that the  $\beta_1$ AR at the SR are not activated at the PM and then translocated to the SR.

### **Activation of the $\beta_1$ AR at the SR promotes optimal cardiac contractility and $\text{Ca}^{2+}$ handling in AVMs.**

Consistent with the PKA activity detected at the SR, sotalol blocked ISO-induced PKA phosphorylation of LTCC at Ser<sup>1928</sup> but did not affect ISO-induced PKA phosphorylation of PLB at Ser<sup>16</sup> in mouse, rat or rabbit AVMs (Online Figure XI). On the other hand, propranolol abolished ISO-induced phosphorylation of PLB and LTCC (Online Figure XI). These data support that activation of the SR- $\beta_1$ AR signaling promotes SR-localized PKA phosphorylation of PLB in AVMs. Accordingly, ISO-induced increases in sarcomere shortening (SS),  $\text{Ca}^{2+}$  transient amplitude and decreases in tau, were partially reduced by sotalol but completely abolished by propranolol in rat AVMs (Figure 5H–J). These data suggest that phosphorylation of PLB by PKA is mediated by localized  $\beta_1$ AR signaling at the SR and promotes myocyte contractility.

Similarly, sotalol selectively inhibited NE-induced PKA activity at the PM yet permitted increases in PKA activity in the SR local domain (Figure 6A–D and Online Figure XIIA–F). We then assessed whether OCT3 controls the NE-induced local PKA activity at the SR in the presence of sotalol. Deletion of OCT3 abolished PKA activity at the SR domain induced by NE in the presence of sotalol (Figure 6A–B and Online Figure XIIA–F). In contrast, ISO-induced PKA activity at the SR was not affected by OCT3KO and sotalol pretreatment (Figure 6C–D). In the presence of sotalol, deleting OCT3 completely blocked NE-induced increases in sarcomere shortening, Ca<sup>2+</sup>transient, and decreases in Ca<sup>2+</sup> decay tau (Figure 6E–G) but did not affect the responses induced by ISO (Figure 6H–J). These data show that in the presence membrane impermeant  $\beta$ -blocker sotalol, NE can selectively stimulate SR- $\beta_1$ AR signaling to promote local PKA activity and enhance myocyte contractility. These activities can be blocked by deletion of OCT3 that is responsible for uptake of NE into AVMs.

### **OCT3 deficiency impairs catecholamine transport in heart and attenuates epinephrine induced inotropy and heart rate in vivo.**

Finally, we sought to understand the impacts of intracellular  $\beta_1$ AR activation on adrenergic regulation of cardiac function *in vivo*. We observed no differences in heart weight/body weight ratios of OCT3KO and WT mice (Figure 7A), indicating a grossly normal cardiac structure in OCT3KO hearts. However, deletion of OCT3 reduced endogenous NE concentration in hearts compared to WT controls, whereas OCT3KO and WT mice had comparable NE concentrations in the plasma (Figure 7B–C). Consequently, OCT3KO mice show lower cAMP concentrations in hearts relative to WT controls (Figure 7D). These data indicate disrupted catecholamine transport and potential intracellular adrenergic receptor activation by OCT3 deletion. Compared to WT, OCT3KO mice showed no difference in cardiac function, including ejection fraction (EF) and heart rate (HR) at baseline conditions (Figure 7E–I). These observations obtained by echocardiography are probably relevant to adaptive gene expressions in myocardium due to OCT3 deletion. The expression of PLB and PLB/SERCA2 ratio were decreased whereas expression of RyR2 was increased in OCT3KO hearts (Online Figure XIII A–B). Furthermore, we detected cardiac  $\beta$ -adrenergic response with 10  $\mu$ g/kg EPI or ISO injection *in vivo*. Compared to WT, OCT3KO mice showed no difference in cardiac function after 10  $\mu$ g/kg ISO administration (Figure 7G–I). However, OCT3KO displayed significantly blunted EF and HR responses to EPI injection relative to WT (Figure 7G–I). These data show that OCT3 is essential for enhancing myocardial contractility induced by epinephrine *in vivo*.

## **DISCUSSION**

Adrenergic signaling is one of the most important mechanisms for regulating cardiac function and is typically blunted/disturbed in cardiac diseases including HF.<sup>23</sup> In this study, we provide evidence to support the presence of a pool of  $\beta_1$ AR at the SR that is essential for enhancing contractility in cardiomyocytes. We also show that monoamine transporter OCT3/EMT mediated catecholamine uptake is essential for activation of the SR- $\beta_1$ AR and for promoting phosphorylation of PLB by PKA and cardiac contractility. Furthermore, our data suggest that different clinically used  $\beta$ -blockers differ significantly in their ability to



suppress internal  $\beta_1$ AR-PKA signaling due to different membrane permeability. While membrane-permeant  $\beta$  blockers such as propranolol and carvedilol are able to block activation of intracellular  $\beta_1$ ARs, membrane impermeant  $\beta$ -blockers such as sotalol and atenolol cannot readily access intracellular  $\beta_1$ AR. Therefore, this study opens a novel avenue to optimize therapeutic strategies for targeting cardiac  $\beta_1$  adrenergic signaling in different clinical settings.

### **Intracellular adrenergic receptor signaling at the SR.**

Accumulating evidence suggests the presence of GPCRs and G proteins inside mammalian cells.<sup>24</sup> Increasing number of intracellular GPCRs have been identified in animal hearts, including angiotensin<sup>3</sup> and adrenergic receptors.<sup>2, 8</sup> In cardiomyocytes, previous studies have characterized both  $\beta_1$  and  $\alpha_1$ ARs, but not  $\beta_2$ AR on the nuclear envelope.<sup>1, 2</sup>  $\beta_1$ ARs were also found to reside in the Golgi apparatus and initiate an internal Gs-cAMP signal from the Golgi apparatus, and this internal signal is independent of receptors at the PM.<sup>7, 8</sup> However, whether ARs are localized at other subcellular locations and their functional implications in cardiac contractility remain to be elucidated. Here, we used a combination of sophisticated molecular probes, genetically modified mice and pharmacological inhibitors to uncover important details of the intracellular  $\beta_1$ AR-cAMP-PKA pathway at the SR. We provide solid evidence of the presence of intracellular  $\beta_1$ ARs at the SR in cardiomyocytes, which is associated with SERCA2 and PLB, consistent with a recent report that exogenously expressed  $\beta_1$ ARs bind to SERCA2 in fibroblasts.<sup>25</sup> Meanwhile, our data do not support the presence of a cardiac  $\beta_2$ AR-SERCA2 complex at the SR membrane. This identification of SR-localized  $\beta_1$ ARs provides a novel possibility to explain precisely compartmentalized  $\beta_1$ AR signaling in cardiomyocytes. Upon  $\beta$ AR activation the locally anchored PKA is activated and promotes phosphorylation of targets within a nanodomain, including LTCC at the PM, PLB on the SR, and troponin I and myosin binding protein C on the myofilaments.<sup>12, 18, 26</sup> The present work shows that activation of the intracellular  $\beta_1$ ARs at the SR is necessary for promoting local PKA activity to phosphorylate PLB and TnI in cardiomyocytes, and probably plays a more critical role in rate-limiting cardiac outputs during the physiological fight-or-flight responses. The intracellular  $\beta_1$ AR and PKA activity was essential to optimize enhancement of  $\text{Ca}^{2+}$  transients and cardiac contractility. Yet, much remains to be learnt about the composition, regulation, and function of this emerging  $\beta_1$ AR signaling machinery at the SR in hearts.

### **Requirement of catecholamine-uptake for intracellular $\beta_1$ ARs activation.**

Based on lipophilicity, different  $\beta$ ARs ligands access intracellular  $\beta_1$ AR either by passive diffusion or transporter-mediated uptake. For instance, the current and prior studies show that hydrophilic catecholamine NE and epinephrine require OCT3/EMT for cellular uptake,<sup>2</sup> whereas hydrophobic ligands (e.g. ISO) can passively cross the PM.<sup>7, 8</sup> During sympathetic stimulation, catecholamine is released from nerve termini to stimulate adrenergic receptors on cardiomyocytes. Extracellular catecholamines are quickly reduced mainly by re-uptake at nerve termini.<sup>27</sup> However, cardiomyocytes can also take up a portion of catecholamines via OCT3/EMT.<sup>28</sup> A key question is raised by these observations: what is the function of the catecholamine uptake into cardiomyocytes? Traditionally, it is considered as a mechanism to clear excess catecholamines to prevent overstimulation of cardiac adrenergic signaling.<sup>14</sup>

However, recent research revealed that intracellular NE activates Golgi-localized  $\beta_1$ ARs to promote PI4P hydrolysis.<sup>8</sup> In this work, for the first time, we show that inhibition of NE uptake by OCT3/EMT reduces intracellular PKA activity at the SR as well as contractility in cardiomyocytes. Accordingly, OCT3/EMT dependent-catecholamine uptake is essential for optimal  $\beta$ AR-induced enhancement of contractility in cardiac muscles. Deletion of OCT3 attenuated EPI-induced increases in cardiac EF. Meanwhile, deletion of OCT3 also blunted EPI-induced increases in cardiac HR, supporting a notion that SR  $\text{Ca}^{2+}$  content contributes to sinoatrial nodal pacemaker cells for physiological heart rate increases.<sup>29</sup> Further studies may be merited to address impacts of intracellular  $\beta_1$ ARs activation on SR  $\text{Ca}^{2+}$  content and  $\text{Ca}^{2+}$  handling in myocytes. It also remains to be examined whether other transporters such as OCT2 may affect activation of intracellular  $\beta_1$ ARs in hearts. These observations highlight the transporter-dependent uptake of catecholamines as a potential drug target for clinical applications in a variety of cardiovascular conditions.

Similarly, clinically used  $\beta$ -blockers differ significantly in their membrane permeability. Carvedilol is a commonly used  $\beta$ -blocker in HF therapy, and it can permeate the PM and inhibit  $\beta_1$ AR at both the PM and intracellular membrane compartments. Thus, it may potentially inhibit detrimental effects of chronic activation of the intracellular  $\beta_1$ AR such as nuclear PKA activity for maladaptive gene expression. In comparison, membrane impermeant  $\beta$ -blockers such as sotalol and atenolol, which should mainly block  $\beta_1$ AR only at the PM,<sup>7, 8</sup> are not widely used for HF therapy. Nonetheless, these  $\beta$ -blockers are effective as anti-arrhythmic drugs,<sup>30</sup> probably in part due to their ability to inhibit  $\beta_1$ AR on the PM. Our study thus provides a conceptual platform to evaluate and assess individual  $\beta$ -blockers for more efficacious therapy in different clinical applications.

### **Integrity of $\beta_1$ ARs at the cell surface and subcellular membrane.**

Recent and previous studies indicate that the activation of intracellular  $\beta$ AR/PKA signal generates localization-specific and substrate specific effects.<sup>7, 8</sup> Membrane localization of  $\beta$ ARs and their associated complexes precisely fine-tune  $\beta$ AR activation, which is essential to maintain the cellular function and appropriate responses to extracellular stimuli, such as catecholamines.<sup>16, 26</sup> More importantly, we found that the integral regulation of  $\beta_1$ AR at both cell surface and the SR is required to achieve maximal enhancement of cardiac contraction via optimally coordinating PKA-dependent phosphorylation of substrates in multiple loci. Impaired integrity of  $\beta_1$ AR/cAMP/PKA signaling and blunted cardiac contractile response to  $\beta$ -adrenergic stimulation have been implicated in pathological stress conditions.<sup>26</sup> It has been reported that in HF  $\beta$ AR activation induced PKA activity is significantly inhibited or abolished at the SR and at the myofilaments, but well-preserved at the PM,<sup>12, 18</sup> suggesting the dysregulation of intracellular  $\beta$ AR/PKA signal is involved in the pathogenesis of HF. Besides, a large body of studies revealed that in human HF, NE reuptake was impaired.<sup>31</sup> Although cardiac NE release by sympathetic nerves was increased in HF patients, cardiac NE uptake and cardiac NE contents were significantly reduced. Accordingly, OCT transporters expression is reduced in dilated cardiomyopathy patients.<sup>15</sup> Those observations are consistent with our findings in OCT3KO mice that disrupted catecholamine uptake leads to decreased NE concentrations and cAMP in the myocardium. Meanwhile, OCT3KO mice show attenuated inotropic response to catecholamines. Taken

together, these findings suggest a decreased activation of intracellular  $\beta_1$ AR at the SR due to dysregulated OCT3 may contribute to the decreased PKA activity and phosphorylation of PLB associated with cardiac dysfunction. The integrity  $\beta_1$ ARs at intracellular membranes and their role in development of HF remains to be further explored.

In summary, this study uncovers a novel signaling paradigm in which a SR-localized intracellular  $\beta_1$ AR is functionally crucial in adrenergic stimulation of cardiac contractility. Moreover, the data not only help to broaden our current understanding of the general role of  $\beta_1$ AR signaling in cardiac regulation, but also open up a novel platform to evaluate and optimize  $\beta$ -blockers in clinical applications based on their “biased” properties in selective inhibition of cardiac  $\beta_1$ AR at distinct subcellular locations.

## Supplementary Material

Refer to Web version on PubMed Central for supplementary material.

## ACKNOWLEDGEMENTS

We thank Johanna Borst and Logan Bailey for isolation of rabbit adult cardiomyocytes, Toni West for manuscript editing, and Mohammad Sahtout for statistical analysis.

### SOURCE OF FUNDING

This work was supported by National Institutes of Health grants R01-HL127764 and R01-HL147263 (YKX), R01-HL133832 and P01-HL141084 (DMB), R01 NS078792, R01-AG055357, and R01-MH097887 (JWH), a VA Merit grant 01BX002900 (YKX), and National Natural Science Foundation of China grant 81700252 (ML). QS is a recipient of American Heart Association postdoctoral fellowship. YKX is an established American Heart Association investigator.

## Nonstandard Abbreviations and Acronyms:

<b>AR</b>	Adrenergic receptors
<b>AVMs</b>	Adult ventricular cardiomyocytes
<b>AKARs</b>	A kinase activity reporters
<b>FL-Prop</b>	BODIPY-tagged propranolol
<b>Ca<sup>2+</sup></b>	Calcium
<b>CORTI</b>	Corticosterone
<b>Dob</b>	Dobutamine
<b>EF</b>	Ejection fraction
<b>EPI</b>	Epinephrine
<b>FRET</b>	Förster resonance energy transfer
<b>FS</b>	Fractional shortening
<b>ISO</b>	Isoproterenol

<b>NE</b>	Norepinephrine
<b>OCT3/EMT</b>	Organic Cation Transporter 3/extraneuronal monoamine transporter
<b>PLB</b>	Phospholamban
<b>PLM</b>	Phospholemman
<b>PM</b>	Plasma membrane
<b>PKA</b>	Protein kinase A
<b>PLA</b>	Proximity ligation assay
<b>RyR2</b>	Ryanodine receptor 2
<b>JP2</b>	Junctophilin 2
<b>SS</b>	Sarcomere Shortening
<b>SERCA2</b>	Sarcoplasmic endoplasmic reticulum Ca <sup>2+</sup> -ATPase 2
<b>SR</b>	Sarcoplasmic reticulum
<b>WT</b>	Wild type
<b>cAMP</b>	Cyclic AMP
<b>OCT3KO</b>	OCT3 knockout
<b>LTCC</b>	L-type calcium channel

## REFERENCES

1. Boivin B, Lavoie C, Vaniotis G, Baragli A, Villeneuve LR, Ethier N, Trieu P, Allen BG and Hebert TE. Functional beta-adrenergic receptor signalling on nuclear membranes in adult rat and mouse ventricular cardiomyocytes. *Cardiovasc Res.* 2006;71:69–78. [PubMed: 16631628]
2. Wright CD, Chen Q, Baye NL, Huang Y, Healy CL, Kasinathan S and O’Connell TD. Nuclear alpha1-adrenergic receptors signal activated ERK localization to caveolae in adult cardiac myocytes. *Circ Res.* 2008;103:992–1000. [PubMed: 18802028]
3. Escobales N, Nunez RE and Javadov S. Mitochondrial angiotensin receptors and cardioprotective pathways. *Am J Physiol Heart Circ Physiol.* 2019;316:H1426–H1438. [PubMed: 30978131]
4. Ibarra C, Vicencio JM, Estrada M, Lin Y, Rocco P, Rebellato P, Munoz JP, Garcia-Prieto J, Quest AF, Chiong M, Davidson SM, Bulatovic I, Grinnemo KH, Larsson O, Szabadkai G, Uhlen P, Jaimovich E and Lavandero S. Local control of nuclear calcium signaling in cardiac myocytes by perinuclear microdomains of sarcolemmal insulin-like growth factor 1 receptors. *Circ Res.* 2013;112:236–45. [PubMed: 23118311]
5. Benard G, Massa F, Puente N, Lourenco J, Bellocchio L, Soria-Gomez E, Matias I, Delamarre A, Metna-Laurent M, Cannich A, Hebert-Chatelain E, Mulle C, Ortega-Gutierrez S, Martin-Fontecha M, Klugmann M, Guggenhuber S, Lutz B, Gertsch J, Chaoulhoff F, Lopez-Rodriguez ML, Grandes P, Rossignol R and Marsicano G. Mitochondrial CB(1) receptors regulate neuronal energy metabolism. *Nature neuroscience.* 2012;15:558–64. [PubMed: 22388959]
6. Revankar CM, Cimino DF, Sklar LA, Arterburn JB and Prossnitz ER. A transmembrane intracellular estrogen receptor mediates rapid cell signaling. *Science.* 2005;307:1625–30. [PubMed: 15705806]

7. Irannejad R, Pessino V, Mika D, Huang B, Wedegaertner PB, Conti M and von Zastrow M. Functional selectivity of GPCR-directed drug action through location bias. *Nature chemical biology*. 2017;13:799–806. [PubMed: 28553949]
8. Nash CA, Wei W, Irannejad R and Smrcka AV. Golgi localized beta1-adrenergic receptors stimulate Golgi PI4P hydrolysis by PLCepsilon to regulate cardiac hypertrophy. *Elife*. 2019;8.
9. Lefkowitz RJ, Rockman HA and Koch WJ. Catecholamines, cardiac beta-adrenergic receptors, and heart failure. *Circulation*. 2000;101:1634–7. [PubMed: 10758041]
10. Xiang Y and Kobilka BK. Myocyte adrenoceptor signaling pathways. *Science*. 2003;300:1530–2. [PubMed: 12791980]
11. Bers DM. Cardiac excitation-contraction coupling. *Nature*. 2002;415:198–205. [PubMed: 11805843]
12. Surdo NC, Berrera M, Koschinski A, Brescia M, Machado MR, Carr C, Wright P, Gorelik J, Morotti S, Grandi E, Bers DM, Pantano S and Zaccolo M. FRET biosensor uncovers cAMP nano-domains at beta-adrenergic targets that dictate precise tuning of cardiac contractility. *Nature communications*. 2017;8:15031.
13. Kawai H, Fan TH, Dong E, Siddiqui RA, Yatani A, Stevens SY and Liang CS. ACE inhibition improves cardiac NE uptake and attenuates sympathetic nerve terminal abnormalities in heart failure. *Am J Physiol*. 1999;277:H1609–17. [PubMed: 10516201]
14. Eisenhofer G The role of neuronal and extraneuronal plasma membrane transporters in the inactivation of peripheral catecholamines. *Pharmacology & therapeutics*. 2001;91:35–62. [PubMed: 11707293]
15. Grube M, Ameling S, Noutsias M, Kock K, Triebel I, Bonitz K, Meissner K, Jedlitschky G, Herda LR, Reinthaler M, Rohde M, Hoffmann W, Kuhl U, Schultheiss HP, Volker U, Felix SB, Klingel K, Kandolf R and Kroemer HK. Selective regulation of cardiac organic cation transporter novel type 2 (OCTN2) in dilated cardiomyopathy. *Am J Pathol*. 2011;178:2547–59. [PubMed: 21641380]
16. Xiang YK. Compartmentalization of beta-adrenergic signals in cardiomyocytes. *Circ Res*. 2011;109:231–44. [PubMed: 21737818]
17. Liu S, Li Y, Kim S, Fu Q, Parikh D, Sridhar B, Shi Q, Zhang X, Guan Y, Chen X and Xiang YK. Phosphodiesterases coordinate cAMP propagation induced by two stimulatory G protein-coupled receptors in hearts. *Proc Natl Acad Sci U S A*. 2012;109:6578–83. [PubMed: 22493261]
18. Barbagallo F, Xu B, Reddy GR, West T, Wang Q, Fu Q, Li M, Shi Q, Ginsburg KS, Ferrier W, Isidori AM, Naro F, Patel HH, Bossuyt J, Bers D and Xiang YK. Genetically Encoded Biosensors Reveal PKA Hyperphosphorylation on the Myofilaments in Rabbit Heart Failure. *Circ Res*. 2016;119:931–43. [PubMed: 27576469]
19. Cui M, Aras R, Christian WV, Rappold PM, Hatwar M, Panza J, Jackson-Lewis V, Javitch JA, Ballatori N, Przedborski S and Tieu K. The organic cation transporter-3 is a pivotal modulator of neurodegeneration in the nigrostriatal dopaminergic pathway. *Proc Natl Acad Sci U S A*. 2009;106:8043–8. [PubMed: 19416912]
20. Jain A, Liu R, Ramani B, Arauz E, Ishitsuka Y, Rangunathan K, Park J, Chen J, Xiang K and Ha J. Probing Cellular Protein Complexes via Single Molecule Pull-down. *Nature*. 2011;473:484–8. [PubMed: 21614075]
21. Brittsan AG and Kranias EG. Phospholamban and cardiac contractile function. *J Mol Cell Cardiol*. 2000;32:2131–9. [PubMed: 11112989]
22. Detroyer A, Vander Heyden Y, Carda-Broch S, Garcia-Alvarez-Coque MC and Massart DL. Quantitative structure-retention and retention-activity relationships of beta-blocking agents by micellar liquid chromatography. *J Chromatogr A*. 2001;912:211–21. [PubMed: 11330791]
23. Lohse MJ, Engelhardt S and Eschenhagen T. What is the role of beta-adrenergic signaling in heart failure? *Circ Res*. 2003;93:896–906. [PubMed: 14615493]
24. Ortiz Zacarias NV, Lenselink EB, AP IJ, Handel TM and Heitman LH. Intracellular Receptor Modulation: Novel Approach to Target GPCRs. *Trends in pharmacological sciences*. 2018;39:547–559. [PubMed: 29653834]
25. Yang Z, Kirton HM, MacDougall DA, Boyle JP, Deuchars J, Frater B, Ponnambalam S, Hardy ME, White E, Calaghan SC, Peers C and Steele DS. The Golgi apparatus is a functionally distinct Ca<sup>2+</sup>

- store regulated by the PKA and Epac branches of the beta1-adrenergic signaling pathway. *Sci Signal*. 2015;8:ra101. [PubMed: 26462734]
26. Bers DM, Xiang YK and Zaccolo M. Whole-Cell cAMP and PKA Activity are Epiphenomena, Nanodomain Signaling Matters. *Physiology (Bethesda)*. 2019;34:240–249. [PubMed: 31165682]
  27. Kvetnansky R, Sabban EL and Palkovits M. Catecholaminergic systems in stress: structural and molecular genetic approaches. *Physiol Rev*. 2009;89:535–606. [PubMed: 19342614]
  28. Obst OO, Rose H and Kammermeier H. Characterization of catecholamine uptake2 in isolated cardiac myocytes. *Mol Cell Biochem*. 1996;163–164:181–3.
  29. Wu Y, Valdivia HH, Wehrens XH and Anderson ME. A Single Protein Kinase A or Calmodulin Kinase II Site Does Not Control the Cardiac Pacemaker Ca<sup>2+</sup> Clock. *Circ Arrhythm Electrophysiol*. 2016;9:e003180. [PubMed: 26857906]
  30. Anderson JL and Prystowsky EN. Sotalol: An important new antiarrhythmic. *Am Heart J*. 1999;137:388–409. [PubMed: 10047618]
  31. Rose CP, Burgess JH and Cousineau D. Tracer norepinephrine kinetics in coronary circulation of patients with heart failure secondary to chronic pressure and volume overload. *J Clin Invest*. 1985;76:1740–7. [PubMed: 4056051]
  32. Liu SB, Zhang J and Xiang YK. FRET-based direct detection of dynamic protein kinase A activity on the sarcoplasmic reticulum in cardiomyocytes. *BBRC*. 2010.
  33. West TM, Wang Q, Deng B, Zhang Y, Barbagallo F, Reddy GR, Chen D, Phan KS, Xu B, Isidori A and Xiang YK. Phosphodiesterase 5 Associates With beta2 Adrenergic Receptor to Modulate Cardiac Function in Type 2 Diabetic Hearts. *J Am Heart Assoc*. 2019;8:e012273. [PubMed: 31311394]
  34. Foulon P and De Backer D. The hemodynamic effects of norepinephrine: far more than an increase in blood pressure! *Ann Transl Med*. 2018;6:S25. [PubMed: 30613600]
  35. Wang Q, Liu Y, Fu Q, Xu B, Zhang Y, Kim S, Tan R, Barbagallo F, West T, Anderson E, Wei W, Abel ED and Xiang YK. Inhibiting Insulin-Mediated beta2-Adrenergic Receptor Activation Prevents Diabetes-Associated Cardiac Dysfunction. *Circulation*. 2017;135:73–88. [PubMed: 27815373]
  36. Reddy GR, West TM, Jian Z, Jaradeh M, Shi Q, Wang Y, Chen-Izu Y and Xiang YK. Illuminating cell signaling with genetically encoded FRET biosensors in adult mouse cardiomyocytes. *J Gen Physiol*. 2018;150:1567–1582. [PubMed: 30242036]
  37. Shi Q, Li M, Mika D, Fu Q, Kim S, Phan J, Shen A, Vandecasteele G and Xiang YK. Heterologous desensitization of cardiac beta-adrenergic signal via hormone-induced betaAR/arrestin/PDE4 complexes. *Cardiovasc Res*. 2017;113:656–670. [PubMed: 28339772]
  38. Pogwizd SM. Nonreentrant mechanisms underlying spontaneous ventricular arrhythmias in a model of nonischemic heart failure in rabbits. *Circulation*. 1995;92:1034–48. [PubMed: 7543829]

## NOVELTY AND SIGNIFICANCE

### What Is Known?

- $\beta_1$ -adrenoceptors ( $\beta_1$ ARs) are the major subtype driving cardiac contractility in response to catecholamine stimulation.
- $\beta_1$ -adrenoceptors ( $\beta_1$ ARs) exist in intracellular membranes.
- Organic Cation Transporter 3 (OCT3) mediates norepinephrine entry into cardiomyocytes.

### What New Information Does This Article Contribute?

- A pool of  $\beta_1$ AR are associated with the sarco-endoplasmic reticulum calcium ATPase (SERCA2) complex at the sarcoplasmic reticulum (SR).
- Activation of the SR localized  $\beta_1$ AR is essential to promote phosphorylation of phospholamban.
- Organic Cation transporter 3 is required for catecholamines (norepinephrine and epinephrine) to enter cells and stimulate the  $\beta_1$ AR at the SR.
- Activation of intracellular SR  $\beta_1$ AR is essential to promote cardiac contractility.

Functional  $\beta_1$ ARs exists at the SR and is critical for PKA-mediated phosphorylation of phospholamban and cardiac contractility upon catecholamine stimulation. Activation of these intracellular  $\beta_1$ ARs requires catecholamine transport via OCT3.

For decades, catecholamines have been shown to signal via  $\beta$ ARs on the plasma membrane to regulate heart contractile functions. Little is known about the presence and function of intracellular  $\beta$ ARs in cardiomyocytes. We show the presence of intracellular  $\beta_1$ AR associated with SERCA2 on the SR. Activation of this SR-localized  $\beta_1$ AR is essential for promoting PKA-dependent phosphorylation of PLB and optimizing the cardiac contraction response. Intracellular  $\beta_1$ AR activation is regulated by catecholamine uptake via the OCT3 transporter or membrane permeant  $\beta$ -blockers in cardiomyocytes. These findings provide new mechanistic insight into the composition, localization and regulation of  $\beta_1$ AR signaling. Targeting intracellular  $\beta_1$ AR and its regulators could have potential therapeutic utility in diseases related to cardiac contractile function.

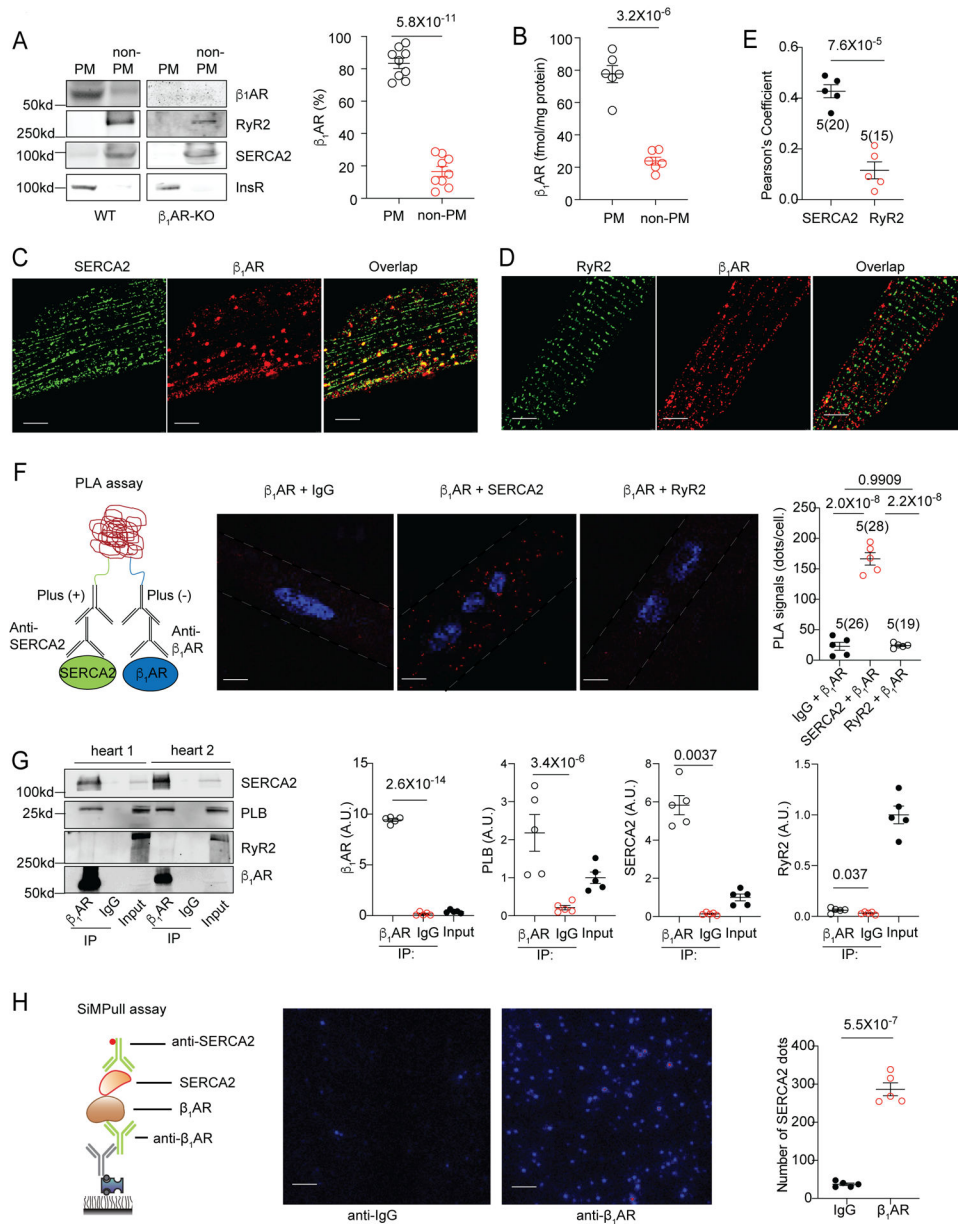


**Figure 1. Intracellular  $\beta_1AR$  associates with SERCA2 but not RyR2 in hearts and isolated mouse adult ventricular cardiomyocytes (AVMs).**

(A) WT and  $\beta_1AR$ -KO mouse heart lysates were fractionated to assess cellular distribution of  $\beta_1AR$ . Representative blots and the percentages of  $\beta_1AR$  in the plasma membrane (PM) and intracellular membrane fractions (non-PM) over the total  $\beta_1AR$  in WT and  $\beta_1AR$ -KO mouse hearts. Data are shown in mean  $\pm$  S.E.M.  $N = 9$  mice.  $p$  values were obtained by student  $t$ -test. (B)  $\beta_1AR$  densities in the PM and non-PM fractions of WT mouse hearts were determined by quantitative radioligand binding assay. Data are shown in mean  $\pm$  S.E.M.  $N = 6$  mice.  $p$  values were obtained by student  $t$ -test. (C-D) Representative confocal images showing distribution of  $\beta_1AR$ , SERCA2, and RyR2 in isolated mouse AVMs.  $\beta_1AR$  was overexpressed in AVMs by infection with recombinant adenovirus. Scale bar = 5  $\mu$ m. (E) The overlap between staining from confocal images was evaluated by Pearson's correlation



coefficient using ImageJ. Data are shown in mean  $\pm$  S.E.M; AVM (in the parenthesis) and mouse numbers are indicated in the figure. p value was obtained by *t*-test. (F) Schematic of *in situ* proximity ligation assay (PLA), exemplary fluorescence images (the whole cell images are in Online Figure II) and quantification of PLA signals after labeling with antibodies against  $\beta_1$ AR and IgG,  $\beta_1$ AR and SERCA2, and  $\beta_1$ AR and RyR2 in AVMs, respectively. Positive PLA signal (red), DAPI (blue). Scale bar = 5  $\mu$ m. Data are shown in mean  $\pm$  S.E.M; AVM (in the parenthesis) and mouse numbers are indicated. p values were obtained by one-way ANOVA followed by Tukey multiple comparison test. (G) Representative images and quantitative assessment of PLB, SERCA2 and RyR2 coimmunoprecipitated with  $\beta_1$ AR in WT mouse hearts. A.U. = arbitrary unit is defined as the ratio of intensity of proteins over inputs. Data are shown in mean  $\pm$  S.E.M. (N = 5); p values were obtained by student *t*-test; (H) Schematic of SiMPull assay and representative images of SiMPull assay after endogenous  $\beta_1$ AR, SERCA2 complex were pulled down with anti- $\beta_1$ AR or control IgG antibodies. The images were quantified using MATLAB. Scale bar = 5  $\mu$ m. Data are shown in mean  $\pm$  S.E.M. N = 5 mice. p values were obtained by *t*-test.

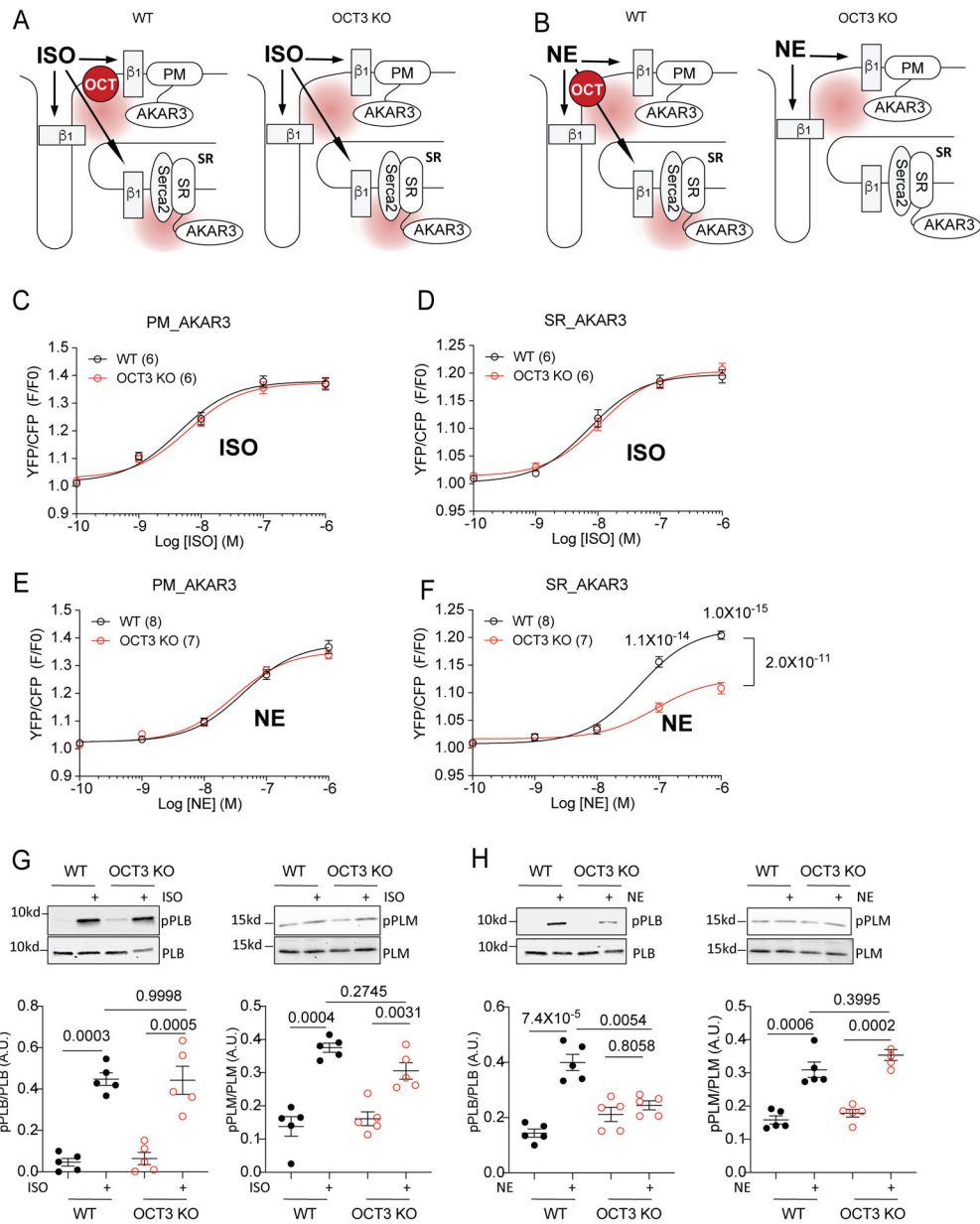


**Figure 2. Differential local regulation of NE-induced  $\beta_1$ AR/PKA activities in WT and OCT3KO AVMs.**

(A-B) Schematics of local activation of  $\beta_1$ AR-induced PKA activity at subcellular locations and detection using FRET based biosensors (plasma membrane, PM-AKAR3 and sarcoplasmic reticulum, SR-AKAR3) in WT and OCT3KO AVMs. Isoproterenol (ISO), norepinephrine (NE). FRET assay was analyzed with F/F<sub>0</sub> of YFP/CFP ratio. (C-D) Concentration-response curves of changes in YFP/CFP ratio after ISO stimulation in WT and OCT3KO AVMs expressing PM-AKAR3 or SR-AKAR3. Data were from 6 WT and 6 OCT3KO mice. (E-F) Concentration-response curves of changes in YFP/CFP ratio after NE stimulation in WT and OCT3KO AVMs expressing PM-AKAR3 or SR-AKAR3. Data were from 8 WT and 7 OCT3KO mice. Data are shown in mean  $\pm$  S.E.M. p values were obtained by two-way ANOVA with Tukey's multiple comparison test when comparing WT to OCT3-

KO. (G-H) Detection of phosphorylation of phospholamban (PLB) at serine 16 and phosphorylation of phospholemman (PLM) at serine 63 in mouse AVMs after stimulation with 100 nmol/L ISO or 100 nmol/L NE. Data are shown in mean  $\pm$  S.E.M. (N = 5). A.U. (arbitrary unit) is defined as the ratio of intensity of phosphorylated proteins over intensity of total proteins. p values were obtained by two-way ANOVA with Tukey's multiple comparison test.

Author Manuscript

Author Manuscript

Author Manuscript

Author Manuscript

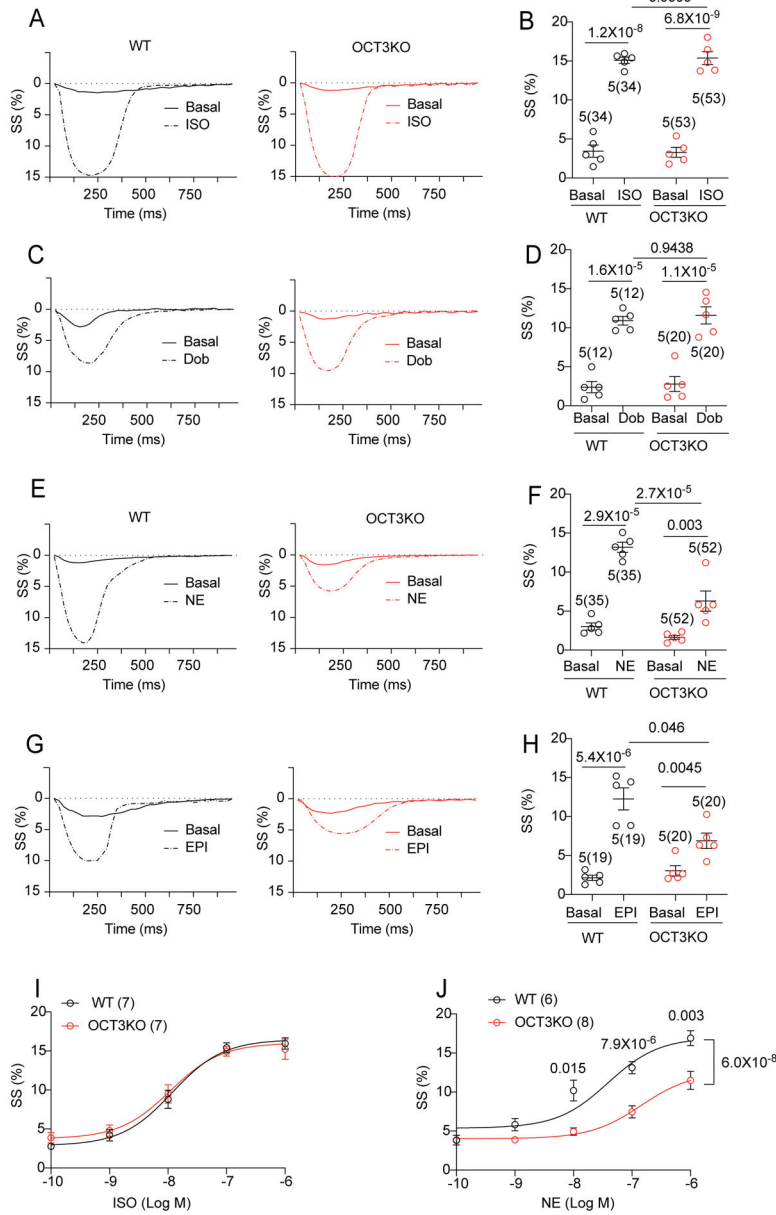


**Figure 3. Deletion of Organic Catecholamine Transporter3 (OCT3) attenuates stimulation of myocyte contractility with norepinephrine and epinephrine.** (A-B) Representative traces show sarcomere shortening (SS) before (close line) and after (dash line) stimulation with ISO (100 nmol/L) in the WT and OCT3KO mouse AVMs. The peak SS were quantified. (C-D) Representative traces show FS before (close line) and after (dash line) the application of dobutamine (Dob, 1 $\mu$ mol/L) in WT and OCT3KO AVMs. The peak SS were quantified. (E-F) Representative traces show SS before (close line) and after (dash line) the application of norepinephrine (NE, 100 nmol/L) in WT and OCT3KO AVMs. The peak SS were quantified. (G-H) Representative traces show SS before (close line) and after (dash line) the application of epinephrine (EPI, 100 nmol/L) in WT and OCT3KO AVMs. The peak SS were quantified. For panel A-H, data are shown in mean  $\pm$  S.E.M. AVM (in the parenthesis) and animal numbers are indicated. p values were obtained by two-way

ANOVA analysis followed with Tukey's multiple comparison test. (I-J) Dose response curves of SS in AVMs after stimulation with ISO (7 WT and 7 OCT3-KO mice) or NE (6 WT and 8 OCT3-KO mice). p values were obtained by two-way ANOVA with Tukey's multiple comparison test when comparing OCT3-KO to WT.

Author Manuscript

Author Manuscript

Author Manuscript

Author Manuscript

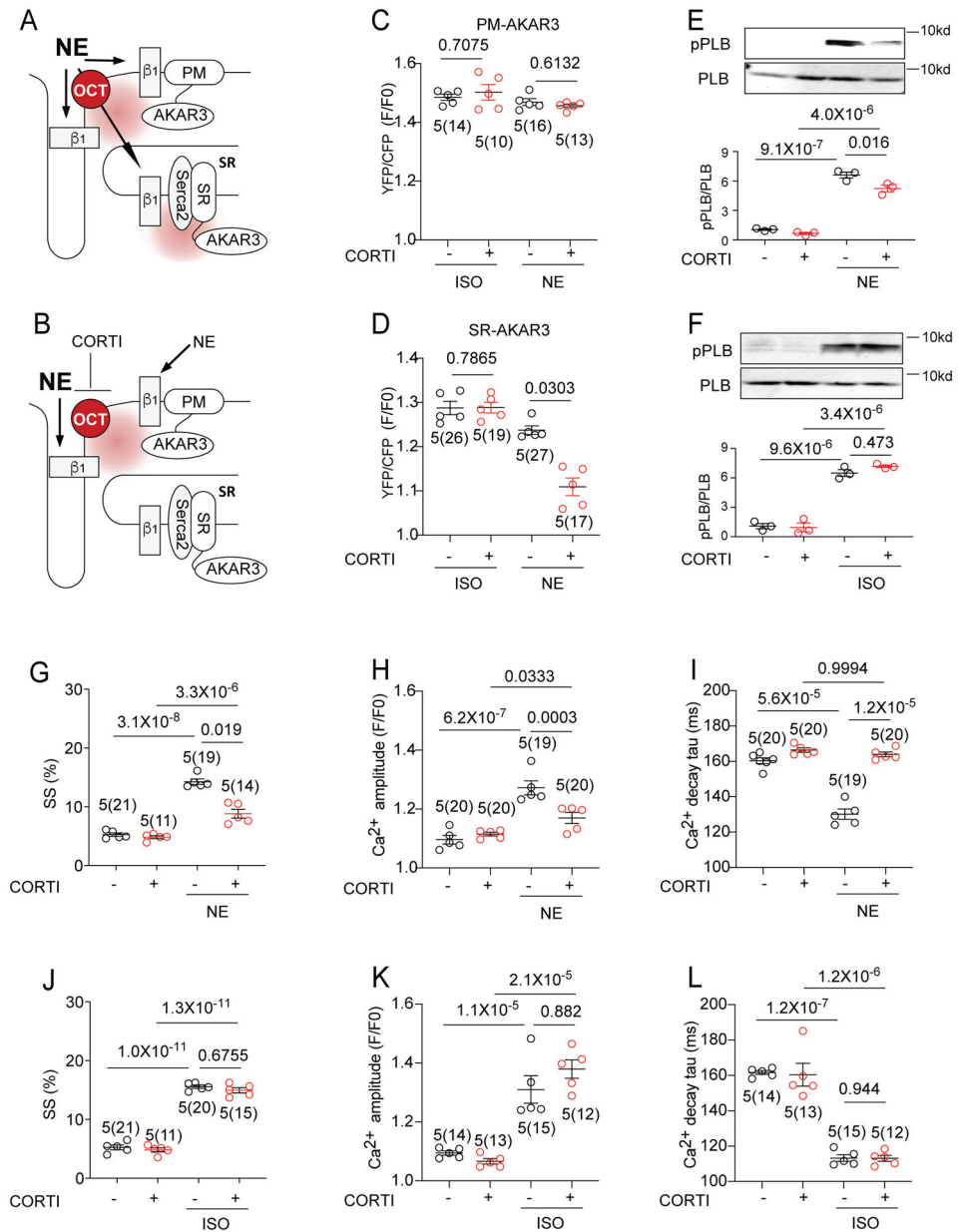


**Figure 4. Inhibition of organic catecholamine transporters reduces norepinephrine-promoted SR-localized  $\beta_1$ AR signal and myocardial contractility.**

(A-B) Schematics show detection of  $\beta_1$ AR-induced PKA activity at different subcellular locations with and without OCT3 inhibitor corticosterone (CORTI). (C-D) Rat AVMs expressing PM-AKAR3 or SR-AKAR3 FRET biosensor were pretreated with CORTI (1  $\mu$ mol/L) before stimulation with NE (100 nmol/L) or ISO (100 nmol/L). FRET was analyzed as F/F<sub>0</sub> of YFP/CFP ratio. Data show the maximal increases in YFP/CFP ratios in mean  $\pm$  S.E.M. AVM (in the parenthesis) and rat numbers are indicated. p values were obtained by One-way ANOVA with Tukey's multiple comparison test. (E-F) Representative immunoblot detection and quantification of phosphorylated serine 16 (pPLB) and total PLB in rat AVMs. Cells were treated with 5-minute incubation with ISO (100 nmol/L) or NE (100 nmol/L) in the absence and presence of CORTI pretreatment. A.U. (arbitrary units) is defined as the

ratio of intensity of phosphorylated proteins over intensity of total proteins. Data are shown in mean  $\pm$  S.E.M. (N = 3). p values were obtained by One-way ANOVA with Tukey's multiple comparison test. (G-L) Rat AVMs were loaded with Ca<sup>2+</sup> indicator, 5  $\mu$ mol/L Fluo-4 AM and pretreated with CORTI (1  $\mu$ mol/L) before stimulation with NE (100 nmol/L) or ISO (100 nmol/L). Sarcomere shortening (SS) and calcium transient amplitude and tau were recorded with 1Hz pacing. Data are shown in mean  $\pm$  S.E.M. AVM (in the parenthesis) and animal numbers are indicated in figures. p values were obtained by One-way ANOVA with Tukey's multiple comparison test.

Author Manuscript

Author Manuscript

Author Manuscript

Author Manuscript

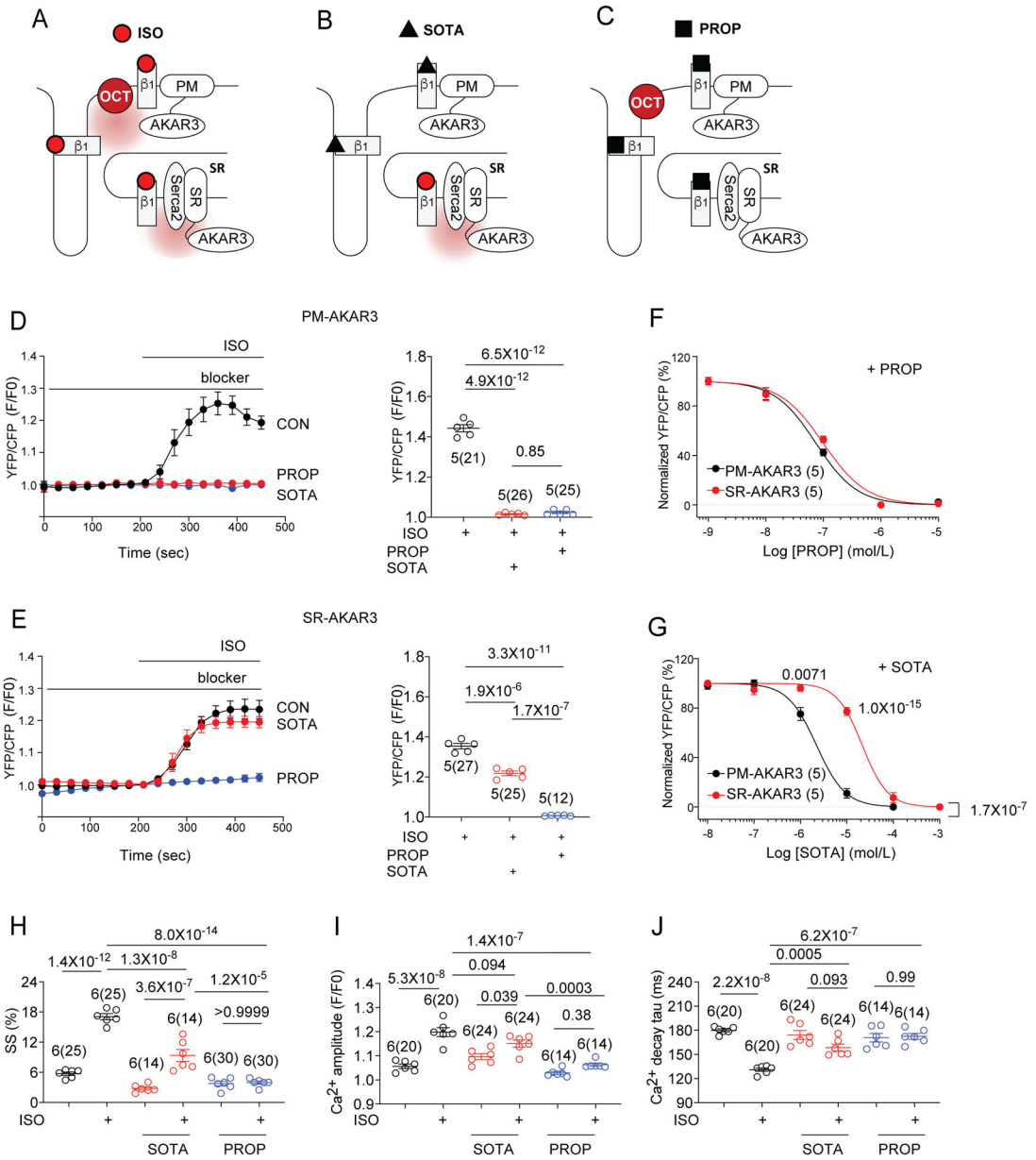


**Figure 5. Activation of  $\beta_1$ AR in the SR is essential for maximal stimulated contractility in AVMs.** (A-C) Schematics show detection of  $\beta_1$ AR-induced PKA activity at different subcellular locations (PM and SR) with FRET based biosensors in the presence of membrane impermeant  $\beta$ -blocker sotalol (SOTA) or the membrane permeant  $\beta$ -blocker propranolol (PROP). (D, E) Rat AVMs expressing PM-AKAR3 or SR-AKAR3 were stimulated with 100 nmol/L ISO with or without 5-minute pretreatment of 25  $\mu$ mol/L SOTA (blue) or 1  $\mu$ mol/L PROP (red). Representative time courses show FRET response of PM-AKAR3 or SR-AKAR3 in AVMs. FRET was analyzed as F/F<sub>0</sub> of YFP/CFP ratio. Data are shown in mean  $\pm$  S.E.M. AVM (in the parenthesis) and rat numbers are indicated. p values were obtained by one-way ANOVA analysis with Tukey's multiple comparison test. (F, G) Dose-dependent inhibition curves of PROP or SOTA on ISO-induced increases in FRET responses in AVMs



expressing PM-AKAR3 or SR-AKAR3. Data show YFP/CFP ratios normalized against the maximal increases induced by ISO in the absence of  $\beta$ -blocker (N = 5 rats). p values were obtained by two-way ANOVA analysis followed by Tukey's multiple comparison test when compared to OCT3-KO. (PM-AKAR3: PROP,  $IC_{50} = 7.399 \times 10^{-8}$  mol/L, SR-AKAR3: PROP,  $IC_{50} = 9.92 \times 10^{-8}$  mol/L; PM-AKAR3: SOTA,  $IC_{50} = 2.216 \times 10^{-6}$  mol/L; SR-AKAR3, STOA,  $IC_{50} = 2.149 \times 10^{-5}$  mol/L). (H-J) Rat AVMs were incubated with  $Ca^{2+}$  indicator (5  $\mu$ M Fluo-4 AM) before 1Hz pacing. After pretreatment with SOTA (25  $\mu$ mol/L) or PROP (1  $\mu$ mol/L), sarcomere shortening (SS) and calcium transient were recorded before and after stimulation with 100 nmol/L ISO. The peak SS, amplitude of  $Ca^{2+}$  transient, and rate of  $Ca^{2+}$  decay (Tau) are shown as mean  $\pm$  S.E.M. Animal numbers and cell numbers are indicated in figures. p values were obtained by one-way ANOVA analysis with Tukey's multiple comparison test.

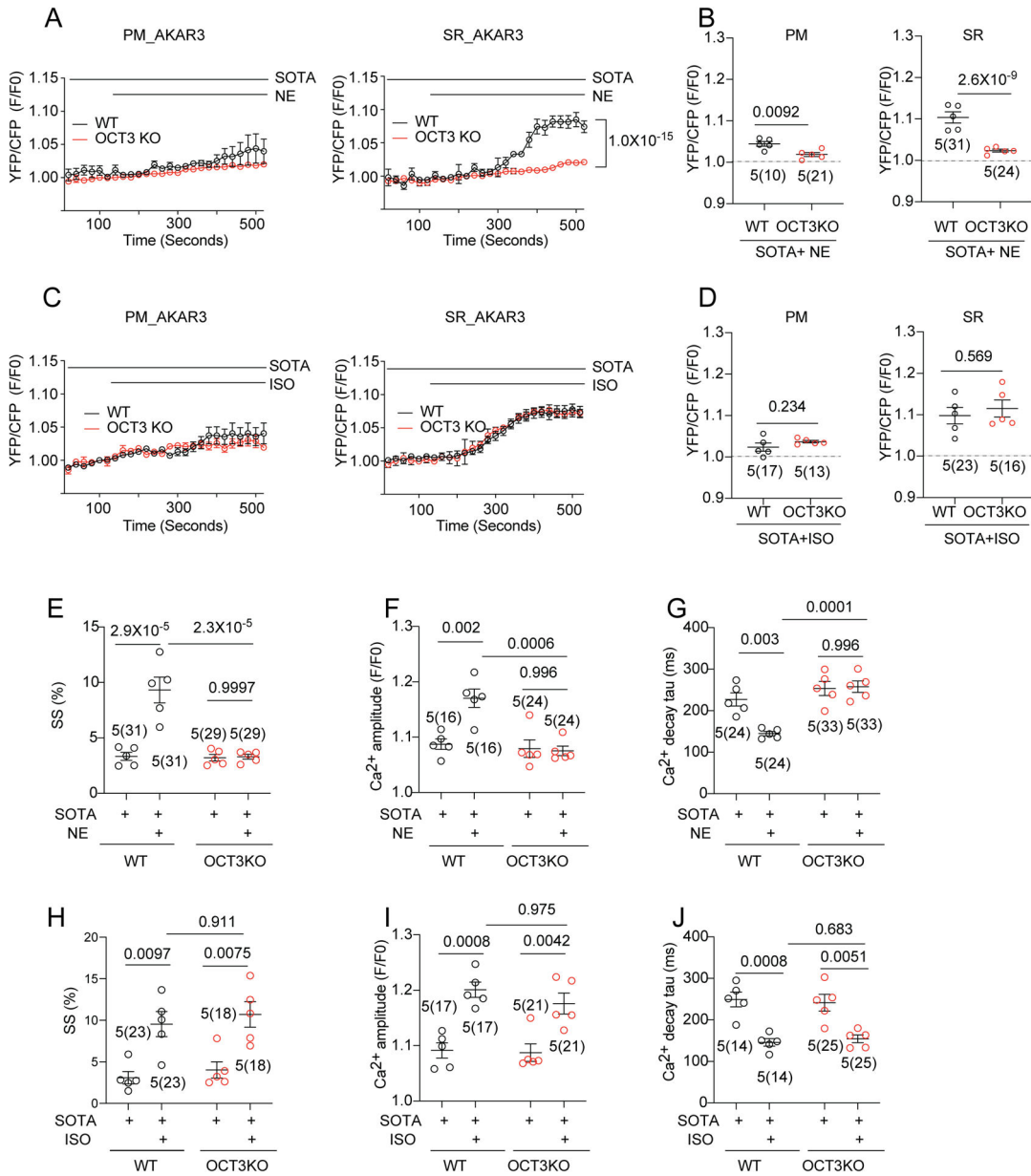


**Figure 6. Activation of  $\beta_1$ AR at the SR promotes myocyte calcium cycling and contractility.** (A, B) WT and OCT3KO AVMs were used to express PM-AKAR3 or SR-AKAR3 biosensors. FRET was analyzed as F/F<sub>0</sub> of YFP/CFP ratio. Representative curves and maximal changes show subcellular PKA FRET responses to NE (100 nmol/L) stimulation in AVMs pretreated with sotalol (SOTA, 25  $\mu$ mol/L). Animal numbers and cell numbers (in the parenthesis) are indicated. p values were obtained by two-way ANOVA analysis followed with Tukey’s multiple comparison test when compared to OCT3-KO. (C, D) WT and OCT3KO mouse AVMs were used to express PM-AKAR3 or SR-AKAR3 biosensors. Representative curves and maximal changes show subcellular PKA FRET responses to ISO (100 nmol/L) stimulation in AVMs pretreated with sotalol (SOTA, 25  $\mu$ mol/L). Animal numbers and cell numbers (in the parenthesis) are indicated. p values were obtained by two-

way ANOVA analysis followed with Tukey's multiple comparison test when compared to OCT3-KO. (E-G) AVMs from WT and OCT3 hearts were stimulated with NE (100 nmol/L) in the presence of SOTA (25  $\mu$ mol/L) pretreatment. Data show maximal changes in sarcomere shortening (SS), Ca<sup>2+</sup> transient amplitude, and rate of Ca<sup>2+</sup> decay (Tau) as mean  $\pm$  S.E.M. Animal numbers and cell numbers (in the parenthesis) are indicated in figures. p values were obtained by two-way ANOVA analysis with Tukey's multiple comparison test. (H-J) AVMs from WT and OCT3 hearts were stimulated with ISO (100 nmol/L) in the presence of SOTA (25  $\mu$ mol/L) pretreatment. Data show maximal changes in SS, Ca<sup>2+</sup> transient amplitude, and Tau as mean  $\pm$  S.E.M. Animal numbers and cell numbers (in the parenthesis) are indicated. p values were obtained by two-way ANOVA analysis with Tukey's multiple comparison test.

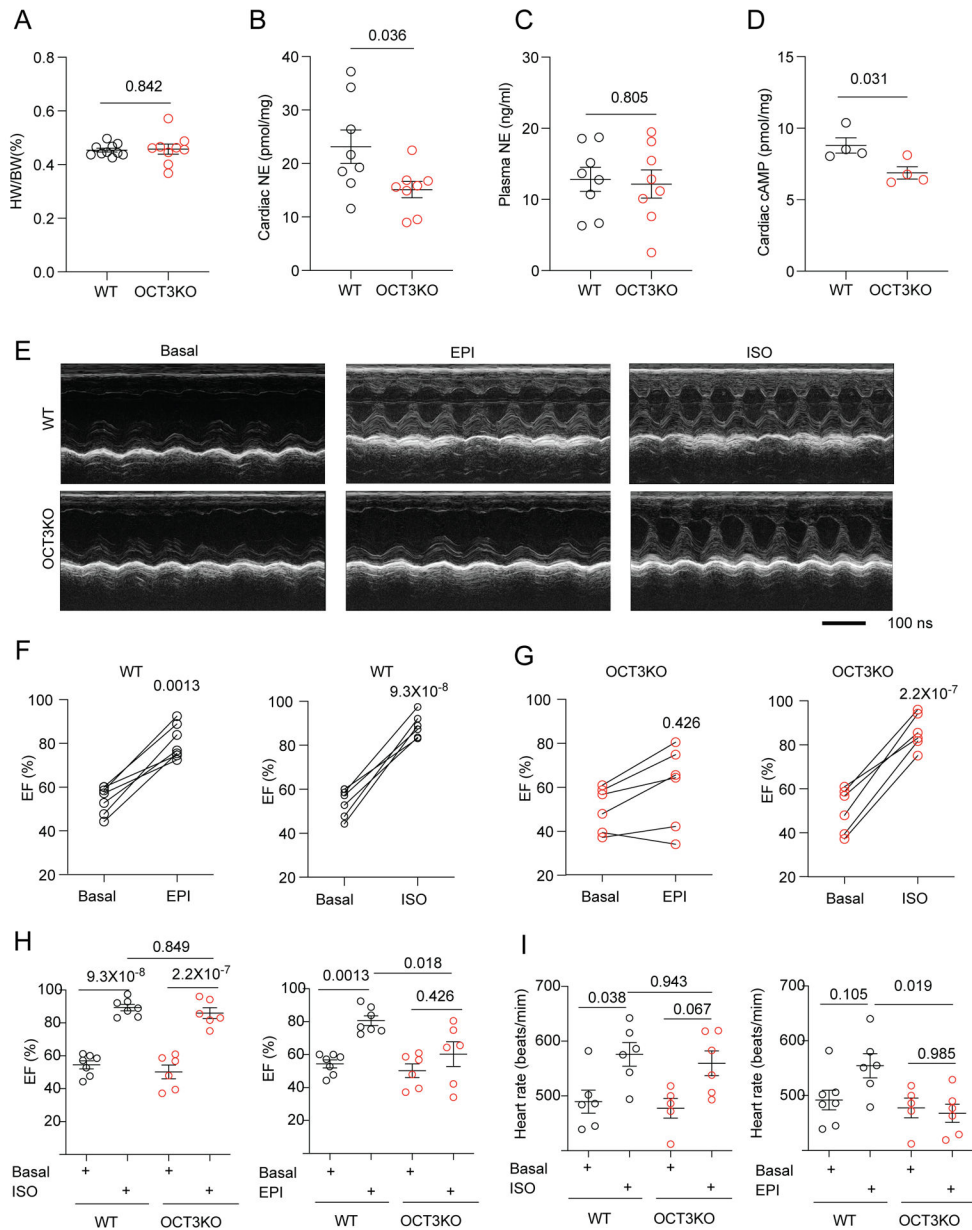


**Figure 7. Deletion of OCT3 reduces catecholamine uptake, cAMP signal and inotropic response in response to adrenergic stimulation of mouse hearts.**

(A) Heart weight/body weight ratio (HW/BW %) in WT and OCT3-KO mice. Data are shown as mean  $\pm$  S.E.M. (N = 8). p values were obtained by student *t*-test. (B, C) Quantitative determination of endogenous NE in cardiac tissues and the plasma. Data are shown as mean  $\pm$  S.E.M. (N = 8). p values were obtained by student *t*-test. (D) Quantitative determination of cAMP levels in cardiac tissues. Data are shown as mean  $\pm$  S.E.M. (N = 4). p values were obtained by student *t*-test. (E) Representative echocardiographic images of WT (N = 7) and OCT3KO (N = 6) mice at baseline and after intraperitoneal injection of 10  $\mu$ g/kg isoproterenol (ISO) or epinephrine (EPI). (F-I) Cardiac ejection fraction (EF) of individual mice before and after intraperitoneal injection of ISO or EPI in WT (N = 7) and OCT3KO (N = 6). Quantification of EF and heart rate (HR) in WT and OCT3KO mice

before and after injection with ISO or EPI. Data are shown as mean  $\pm$  S.E.M. p values were obtained by two-way ANOVA analysis with Tukey's multiple comparison test.

Author Manuscript

Author Manuscript

Author Manuscript

Author Manuscript